

## Closing the gap between research and practice in EM data interpretation

Douglas W. Oldenburg\*, Roman Shekhtman, Rob A. Eso, and Colin G. Farquharson, University of British Columbia–Geophysical Inversion Facility, Perry Eaton, Bob Anderson and Brock Bolin, Newmont Mining Corporation.

### Summary

Electromagnetic data from a CSAMT survey consisting of two transmitter electrodes and multiple frequencies are inverted to generate a 3D distribution of electrical resistivity. The results are compared with those from a 2D inversion which assumes the data are in the far field, and to a 3D resistivity model obtained by inverting DC resistivity data. CDI resistivity images and results from 1D inversions of time domain EM data are also included for comparison. The data are acquired from Antonio, a high sulfidation gold deposit in the Peruvian Andes. The consistency between the 3D images shows that we are making substantial progress in reducing the gap between state-of-the-art research and practical implementation of inversion codes and interpretation of EM data.

### Introduction

Estimating the distribution of resistivity is an important step in many exploration campaigns. Different types of geophysical surveys and interpretation methods provide information about this parameter, however when we compare the results from a DC/IP survey with an airborne EM or a CSAMT survey, or when we compare 2D versus 3D inversion results for the same survey, the “pictures” that emerge are often inconsistent. In the last few years considerable advances in geophysical inversion have been made so that we now have the capability to invert most types of survey data to recover a 3D resistivity distribution. Yet we are still in the early stages of applying these techniques to field data sets and to verifying the results. In this paper we focus upon the Antonio deposit in Peru for which CSAMT, DC/IP and airborne time domain data have been collected. We begin with background about the deposit and the survey data and then present the inversion results.

### Geologic Background

The main alteration control at the Antonio deposit is the intersection of NNE and EW trending faults where phreatic and hydrothermal breccias were forced upwards through the volcanic pile. The gold mineralization is mostly confined to massive silica, vuggy silica, and granular silica alteration found along these structures, which probably represent the feeder mechanism for the system. Additional mineralization is found as crackle breccia in the host rock if it had sufficient pore space for hydrothermal fluids to permeate and deposit gold. Later structures striking N45W crosscut the NNE and

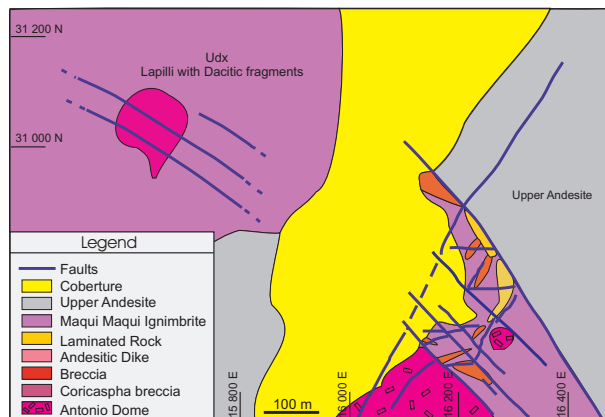


Fig. 1: Antonio Geology, Peru.

EW faults but are post-mineralization. Figure 1 shows the surface lithologies and structures in the main area of interest (?). The fault-bounded, arc-shaped zone of laminated and brecciated rock corresponds to the outcrop of the deposit.

### Survey Data

Several electrical and electromagnetic surveys were carried out over the Antonio property in order to map the high resistivity associated with silicification. In general, highly resistive rock represents direct drill targets in this environment. Initial shallow drilling proved to not be particularly encouraging, in line with what came out of 2D inversion of the initial geophysics, i.e. pole-dipole DC/IP lines. In fact the overall interpretation was one of a thin “scab” of alteration and for a while the property was dismissed as lacking potential. Fortunately, a couple of deeper holes indicated the presence of high grade material and subsequently CSAMT and airborne EM surveys were carried out in order to refine the geological model and to focus the drilling effort.

The pole-dipole lines (Figure 2) consist of conventional IP/resistivity data acquired using an in-house crew and Hunttec/Iris equipment. The lines trend east-west and are about 150 meters apart with 50 meter stations. Quantec acquired conventional asynchronous scalar CSAMT data with 50 meter stations on 150 meter spaced east-west or north-south lines. The airborne data were acquired using NEWTEM, a proprietary time-domain helicopter EM system developed and operated by Newmont (?). The airborne EM data were acquired as part of a much larger sur-

## Closing the gap in EM data interpretation

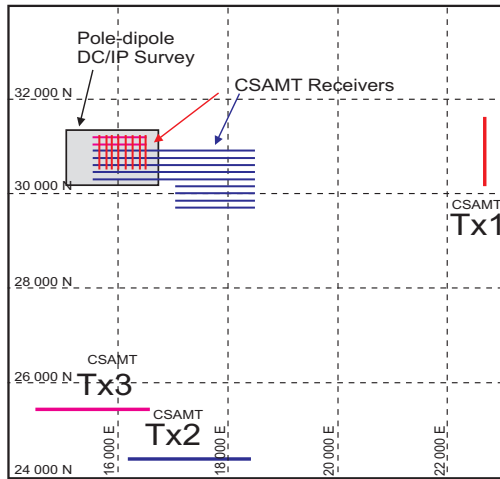


Fig. 2: Antonio Geophysical Survey Map.

vey of the Yanacocha district. In this case data were acquired on east-west profiles spaced 200 meters apart. The additional geophysics provided indications of the presence of mineralization at depth. However the combination of 1D, 2D and 3D interpretations of these data sets was not consistent. Three different CSAMT transmitter sources were employed (Figure ??) in order to try to resolve why the 2D results from any one of these surveys did not meet our expectations based on limited drilling information. Prior to taking a 3D approach with the CSAMT interpretation, we believed that the CDI-style interpretation of the airborne EM data provided the best “footprint” for the known mineralization at depth.

### CSAMT Surveys

For the first attempt at extracting information from the CSAMT data, a 2D MT inversion code was used. This work was done at Newmont and made use of Zonge software called SCS2D. This approach assumes that the area of interest is in the far-field of the transmitters, that is, a number of skin depths away. Using a representative resistivity of 50  $\Omega\text{m}$ , this limits the useable frequencies to be higher than about 32 Hz. Because of the 2D assumption, data for the different transmitters needed to be inverted independently. Frequencies 32–8196 Hz were inverted for the eight north-south lines and the results for Tx1 are shown in Figure 3a where the purple areas are less than 100  $\Omega\text{m}$  and the red areas are in excess of 1000  $\Omega\text{m}$ . The 2D inversion results have been composited into a 3D model and this is a planview plot of resistivity interpolated from that model 100 meters below the surface. A similar procedure was applied to seven of the east-west lines of data (Tx2 & Tx3), and a resistivity slice at 100 meters depth is shown in Figure 3b. Note that the resistive features highlighted in these maps do not spatially coincide. By inverting single-source scalar data without the low frequency content, there are some obvious limitations. To obtain further insight, it was

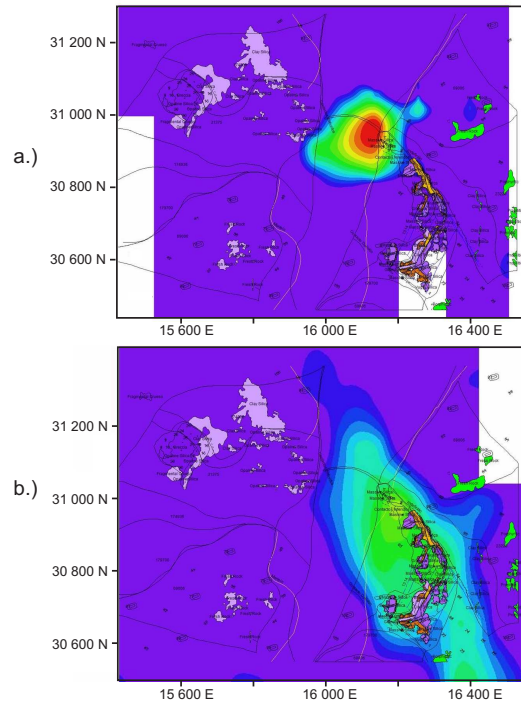


Fig. 3: 2D CSAMT Resistivity Model. a.) Tx1. b.) Tx2 and Tx3.

decided to invert the data with a 3D algorithm.

The inversion algorithm, EH3Dinv, is a Gauss-Newton algorithm which is described in Haber et al. (?). It is a finite volume based code that can generate a 3D conductivity distribution from multiple transmitter locations. The earth is gridded into rectangular prisms, each of which has a constant, but unknown conductivity. In order for the numerical modeling to be accurate, the size of the cells needs to be considerably smaller than the skin depth of the EM wave. Thus, for frequencies of 100Hz, the cell size should be about 100 meters. This presents difficulty for the CSAMT configuration where the transmitter is at a large distance because, to model both the transmitter and survey area, a large number of cells is required. For instance, if the cell dimension is 100 meters, we need about  $10^6$  cells. But even 100 meter cells are too coarse in the region of interest; there cells sizes of 50 meters or less are more appropriate. With our currently available computing power, we can work with meshes that have about  $10^5$  cells.

To deal with the above problem we took a 2-step procedure. In the first we meshed the entire volume, including topography, with 200 meter cells and assigned a constant resistivity of 50  $\Omega\text{m}$  to the volume. A forward modeling was carried out and we computed the electromagnetic fields on the boundary of an interior volume which enclosed the region of interest. Those fields were used as boundary conditions for inverting data inside this region. Because the domain is smaller, the area underlying the survey stations can be meshed with 50 meter cells. The

## Closing the gap in EM data interpretation

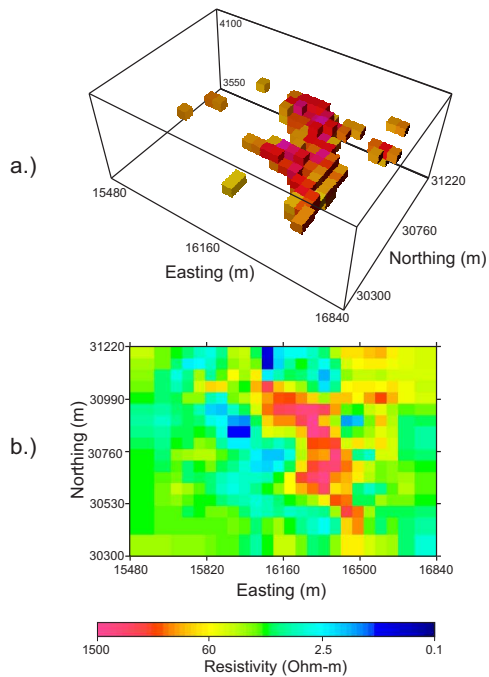


Fig. 4: CSAMT Resistivity Model. a.) iso-surface, 83  $\Omega\text{m}$  cutoff. b.) planview, depth 3900 m.

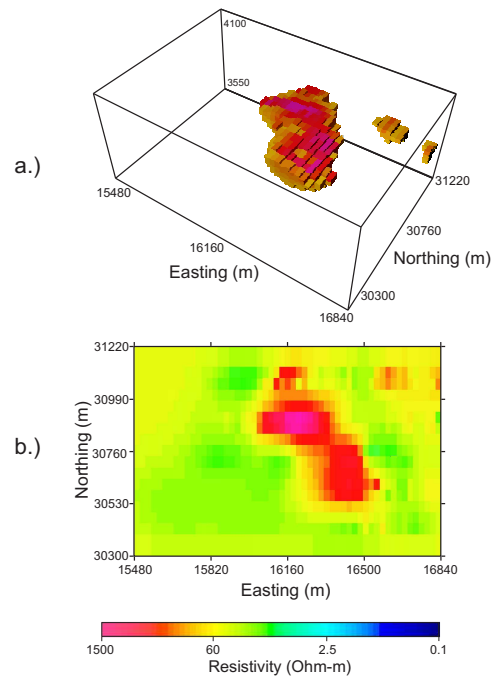


Fig. 5: 3D DC resistivity model. a.) iso-surface, 83  $\Omega\text{m}$  cutoff. b.) planview, depth 3900 m.

total number of cells in the final inversion was 73,226.

The crucial step of estimating uncertainties to the data was done in an empirical manner. Amplitude and phase data at 4 Hz and 64 Hz were viewed and we sought values for the standard errors that would be small with respect to major variations of signal across the data set, and yet large compared to station to station fluctuations. This led to rules of 10% and 2 degrees for the standard deviations of the amplitude and phase respectively. To obtain some confidence that this was reasonable, we first inverted data from each transmitter and at each frequency separately. The results for simultaneously inverting data from Tx1 and Tx2 at frequencies 4 Hz and 64 Hz are given in Figure 4. The plan view map shows a major resistive unit that collocates with the resistive features shown in the 2D CSAMT inversions. An iso-surface image of the resistor is also shown in this figure. These images allow us to understand the 2D inversions. Each 2D inversion sees a portion of the resistor to which it is best coupled. In this case the information about the resistor is in the electric field and is most evident when the strike of the main zone of silification is perpendicular to the direction of the transmitter.

### DC/IP Inversion

The DC resistivity data were inverted using a modified version of DCIP3D (?). The main improvement to the code has been to remove the limitation that the current and potential electrodes be at the nodes of the mesh. In

areas of large topography like Antonio, this has proved to be very practical and has allowed us to run the inversion using fewer cells than would have been the case in the past. The volume of interest was divided into 36,000 cells. We assigned data errors of 12.5% plus a baseline of 5 millivolts. A planview resistivity section and an iso-surface image are shown in Figures 5. The good agreement between CSAMT and DC results is extremely gratifying.

### 1D analysis of airborne TEM

Reconnaissance airborne time-domain EM data were acquired over the area using Newmont's NEWTEM system. The data were processed at Newmont and also converted to CDI images with their proprietary software (?). This approach imposes no specific model and is effectively a point-by-point transformation of transient decays (field versus time) into resistivity versus depth profiles. The data have also been inverted using a new 1D time-domain inversion code, EM1DTM (the time-domain version of program the EM1DFM, Farquharson et al, 2002). In either case, each sounding is processed separately and the results are stitched together to make a 2D or 3D image. In the 1D inversion approach, the Earth was divided into 81 layers. For comparison purposes we look at the resultant resistivities obtained from 1D inversion and CDI imaging, and from 3D DC inversion and CSAMT inversion, along an east-west transect that cuts through the area of interest. All results in Figure 6 are plotted on the same color scale. The white

## Closing the gap in EM data interpretation

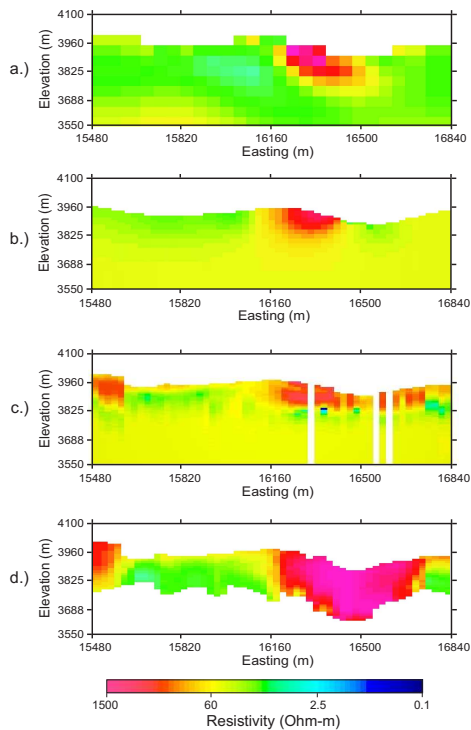


Fig. 6: Cross sections along 31,000 N: a.) CSAMT. b.) DC resistivity. c.) 1D EM Inversion. d.) CDI.

lines for EM1DTM correspond to soundings that were problematic in the inversion. To first order, the images convey a consistent message about the resistive structure and, in particular, the existence of the resistive target near 16300 m E. At the more detailed level, differences are due to a combination of effects: the methodology associated with the measurement of fields that reflect the distribution of resistivity and the means by which we extract that information from the measurements.

### Conclusion

In this work we present one of the first rigorous inversions of 3D controlled source EM data for field data. The results are compared with those from 3D inversion of DC resistivity data and from 1D imaging and inversion results for time domain EM data. There is general correspondence of major resistive features observed in all three data sets but details are different. The inversions provide insight about a number of items. First, 2D CSAMT analysis using a single transmitter, and restricting frequencies so that the receiver is in the far field, can produce results of limited usefulness. Also, a major amount of insight about the structure is available from low frequency fields and even information at a single frequency and from two transmitters can provide substantial information. In this exercise involving asynchronous data, we became keenly aware of the disadvantage of not being able to work directly

with properly referenced electric and magnetic fields. We strongly recommend that synchronous field data be acquired. By moving the transmitters in closer to the area of interest and consequently committing to a full 3D inversion, one can likely increase the signal-to-noise in the data. It seems apparent that surveys consisting of a few judiciously-placed, nearby transmitters and orthogonal field components at a few frequencies can provide a data set from which significant information about the subsurface can be extracted. Lastly, our fast CDI imaging and 1D inversion approaches show good promise for identifying the main areas of interest and supplying information about a background resistivity that can be used in 3D analysis.

### Acknowledgements

We thank Newmont Mining Corporation for permission to discuss our work on the Antonio project. In particular we would like to acknowledge the support and encouragement offered by Lewis Teal, Director of Exploration at Yanacocha. We thank Jiuping Chen and Peter Lelievre for their assistance is working with the CSAMT data. The work at UBC-GIF was supported by the TIME Consortium whose members include: Placer Dome, Teck-Cominco, Noranda-Falconbridge, Newmont Gold, INCO, ENI, Anglo-American and Rio Tinto.

### References

- Eaton, P., Anderson, R., Nilsson, B., Lauritsen, E., Queen, S., and Barnett, C., 2002, Newtem - a novel time-domain helicopter system for resistivity mapping: 72nd Annual Int'l Meeting of the Soc of Exp Geop, Salt Lake City, Utah, October 6-11.
- Eaton, P., 1998, Application of an improved technique for interpreting transient electromagnetic data: *Exploration Geophysics*, **29**, 175-183.
- Farquharson, C. G., Oldenburg, D., and P.S., R., 2003, Simultaneous 1d inversion of loop-loop electromagnetic data for magnetic susceptibility and electrical conductivity: *Geophysics*, **68**, 1857-1869.
- Haber, E., Ascher, U., and Oldenburg, D., 2004, Inversion of 3d electromagnetic data in frequency and time domain using an inexact all-at-once approach: *Geophysics* (in press).
- Li, Y., and Oldenburg, D., 2000, 3-d inversion of induced polarization data: *Geophysics*, **65**, 1931-1945.
- Pinto, R., and Quispe, J., 2003, Antonio project: Exploration and development final report: Minera Yanacocha Exploration Geology Department.